Macromolecules

pubs.acs.org/Macromolecules Article

Synthesis of Hydrophilic Thermoplastic Elastomer with Outstanding Mechanical Properties via the Copolymerization of Ethylene and Methoxystyrene

Hui Tian, Chunji Wu, Baoli Wang,* and Dongmei Cui

Cite This: *Macromolecules* 2025, 58, 6844−6853 Read Online

ACCESS | Metrics & More | Article Recommendations | Supporting Information

ABSTRACT: Polyolefin thermoplastic elastomers are of fundamental interest and practical importance. Herein, we report the copolymerization of ethylene (E) with three kinds of styrene derivatives (*ortho*-methoxystyrene (*o*MOS), *meta*-methoxystyrene (*m*MOS), and *para*-methoxystyrene (*p*MOS)) using two kinds of heterocyclic-fused cyclopentadienyl scandium complexes **1** and **2**. E-*o*MOS copolymer products with glass-transition temperatures (T_g) higher than room temperature behave as hard plastics, while E-*m*MOS copolymers are thermoplastic elastomers with lower T_g values (−13 to −23 °C). E-*m*MOS copolymers have higher number-averaged molecular weight (M_n 4.7−11.6 g mol^{-1}) and show excellent mechanical properties due to the unique multiblock-like chain structures composed of relatively long crystalline E−E segments as hard parts and short amorphous *m*MOS-*m*MOS sequences as soft parts. The chain and phase structures of E-*m*MOS copolymers have been studied by nuclear magnetic resonance (NMR) spectra, atomic force microscopy (AFM), and wide-angle X-ray diffraction (WAXD) analysis. Incorporation of *m*MOS groups endows materials with improved hydrophilic surface properties and high mechanical properties.

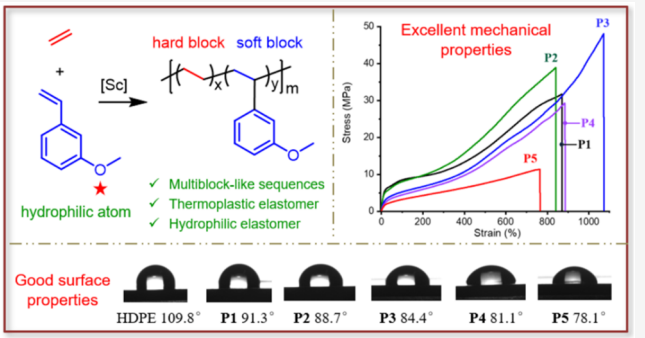

INTRODUCTION

Thermoplastic elastomers (TPEs) possess the classical elastic characteristic like thermoset rubbers and can be easily processed like thermoplastics, which is distinct with common rubbers.[1,2] Traditional vulcanized rubbers containing chemical cross-links are difficult to reprocess and reuse and have brought large amounts of wastes into human daily life.[3,4] TPEs have a lot of advantages, such as recyclability, low density, high chemical resistance, and ease of manufacture using common processing techniques. They have become a potential alternative to vulcanized rubbers to meet the requirements of the sustainable circular economy for the new generation of synthetic elastomers.[5] Commercially available TPEs are an important class of polymeric materials and divided into several categories based on their constituent elements, including thermoplastic polyurethanes (TPUs), styrenic block copolymers (SBCs, such as styrene-butadiene-styrene (SBS) copolymer), polyolefin thermoplastic elastomers (TPE-Os), *etc.*[6] Despite the difference in their chemical components, TPEs are blocky copolymers composed of "soft" segments (offering elastic recovery) and "hard" snippets (providing physical cross-linked points) in principle.[7] TPUs consist of polylol parts (soft) and polyisocyanate parts (hard),[8] while SBSs contain polybutadiene segments (soft) and polystyrene ones (hard).[9]

TPE-Os are the charming TPEs due to their high-performance, resistance to chemicals, and sufficient supply of olefin monomers (such as ethylene), and have been widely used in the production of automotive components, building and construction, cables, *etc.*[10,11] Commercially available polyolefin elastomers (POEs) are ethylene/α-olefin copolymers with random α-olefin distribution, and are the largest volume of TPE-Os.[12] α-Olefin incorporation into polyethylene (PE) chains provides several soft segments, while residual long PE parts are hard segments.[13] POEs are block-like copolymers, but these random molecular microstructures form nonuniform soft and hard segments, and therefore, their mechanical properties are limited. Olefin block copolymers (OBCs) subsequently emerged via the copolymerization of ethylene (E) and 1-octene catalyzed by two different catalysts in the presence of chain-transfer agent (CTA) through the "chain-shutting" mechanism.[14] These blocky molecular microstructures give crystallizable (low content of 1-octene) and

Received: April 9, 2025
Revised: June 18, 2025
Accepted: June 20, 2025
Published: June 25, 2025

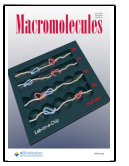

https://doi.org/10.1021/acs.macromol.5c00949
Macromolecules 2025, 58, 6844−6853

Scheme 1. Copolymerization of Ethylene and Functionalized Styrene Catalyzed by Transition Metal Complexes

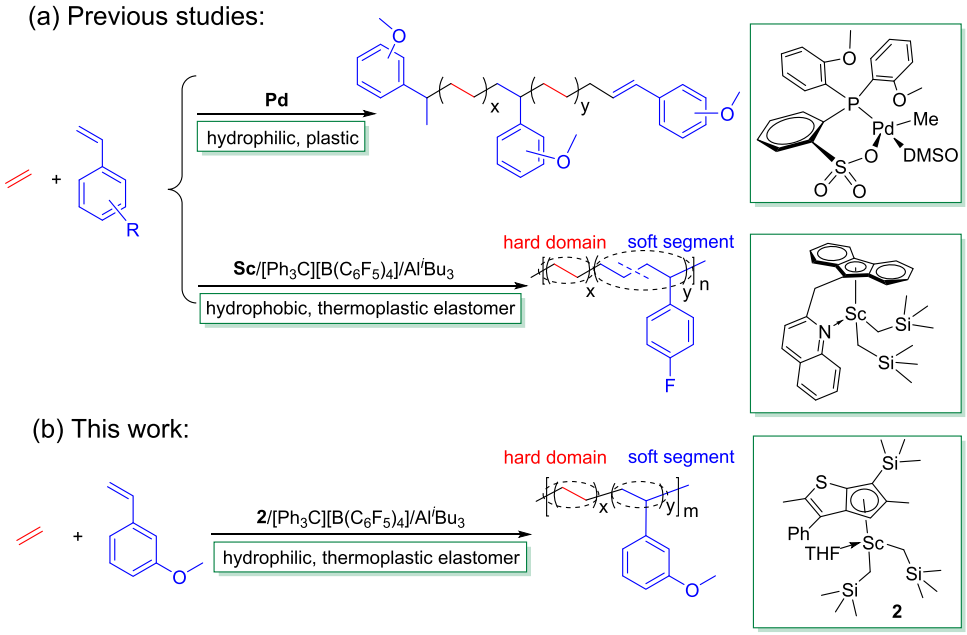

noncrystallizable (low content of ethylene) alternative statistical hard/soft segments in a uniform fashion, and give OBCs superior mechanical performances compared with POEs.[15] Since then, many efforts have been devoted to searching for new catalytic systems to create new multiblock-like copolymers.[16−20] However, the practical effects are limited due to the difficulty encountered in finding new and efficient catalyst combinations (two kinds of catalysts and CTA). Design and synthesis of new TPEs with uniform multiblock-like chemical microstructure by using one catalyst in a controllable fashion is an attractive subject for both academia and industry and has remained a challenge to date.

On the other hand, traditional POEs and OBCs consist of only carbon and hydrogen atoms, leading to poor surface properties, adhesion, dyeability, conductivity, and compatibility with processing auxiliary reagents and other polar materials, which restrict their application in specific environments.[21−23] Then, hydrophilic modification was performed via the graft functionalization of POEs using peroxides at harsh stirring mechanical conditions under high temperatures in an uncontrollable fashion.[12,24−27] The direct coordination copolymerization of ethylene with hydrophilic monomers is, in principle, the most straightforward, atom- and energy-efficient methodology to synthesize hydrophilic TPEs compared with other strategies. The coordination copolymerization of ethylene with polar monomers catalyzed by late transition metal catalyst systems has been reported, but the polar olefins incorporation was low,[28] and most of the resultant copolymers are not elastomers.[29] Jian et al. reported the synthesis of a series of ethylene/polar styrene copolymers by using a neutral phosphine-sulfonate palladium complex (Scheme 1(a)). The resultant copolymers have low polar styrene incorporation (<6.3 mol %), and all of them are plastics.

Organo-scandium complexes could serve as efficient catalysts for the copolymerization of ethylene and heteroatom-containing styrene (St′) via heteroatom-assisted strategy, giving copolymers with random, discrete {-EE(St′)EE-} and alternating sequences {-E(St′)E(St′)E-} structures.[30,31] Moreover, the heterocyclic scandium complexes have exhibited better catalytic performance toward heteroatom-containing olefins,[32−34] because these novel ligands could change the Lewis acidity of the central metal and thereby weaken the poisoning effect of polar monomers on catalysts.[35] However, the resultant copolymers are also plastomers. Cui et al. made a breakthrough and reported the synthesis of a new elastomer containing hydrophobic groups via the copolymerization of ethylene with fluorostyrene (Scheme 1(b)).[36] These copolymers were composed of soft ethylene-fluorostyrene segments and hard crystalline ethylene−ethylene segments with the isolated fluorostyrene on PE chains and exhibited excellent mechanical properties. These results encouraged us to check whether scandium catalysts could synthesize hydrophilic TPEs.

Herein, for the first time, we report the direct synthesis of hydrophilic TPEs via the copolymerization of ethylene and methoxystyrene (St^O) catalyzed by heterocyclic-fused cyclopentadienyl scandium catalysts (Figure 1), fielding E-St^O

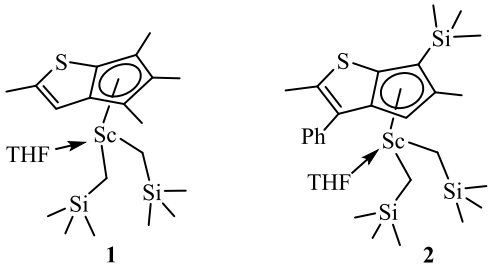

Figure 1. Structures of thiophene-fused cyclopentadienyl scandium complexes **1** and **2**.

copolymers containing different lengths of ethylene segments divided by short continuous St^O−St^O units. Different lengths of ethylene segments show different crystallization behaviors (showing two obvious T_m's) and are hard segments, while short continuous St^O−St^O units are soft segments. These novel multiblock-like hard/soft microstructures make copolymers behave like TPEs at room temperature and show outstanding mechanical properties. The microstructure analysis, morphol-

https://doi.org/10.1021/acs.macromol.5c00949
Macromolecules 2025, 58, 6844−6853

Table 1. Copolymerization of Ethylene with *ortho*-Methoxystyrene Catalyzed by Scandium Complexes 1 and 2[a]

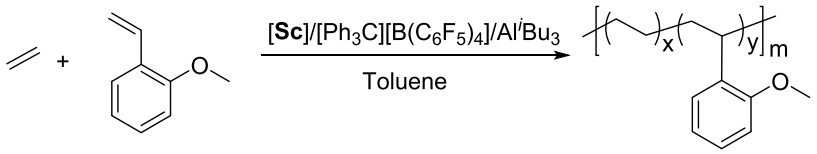

entry	Sc	[M]/[Sc]	yield (g)	Act.[b]	f_M[c] (mol %)	M_n[d] (×10⁴)	M_w/M_n[d]	$M_{n,calcd}$[e] (×10⁴)	T_g[f] (°C)	T_{m1}[f] (°C)	T_{m2}[f] (°C)
1	**1**	100	0.23	0.34	14.3	6.2	1.1	2.3		135	
2	**2**	100	0.56	0.83	30.3	5.8	1.1	5.6	83	135	241
3	**1**	200	0.34	0.50	31.5	10.9	1.2	3.4	84	136	245
4	**1**	300	0.48	0.71	48.2	11.2	1.1	4.8	86	133	241
5	**1**	400	0.87	1.29	69.0	29.0	1.1	8.7	88	133	241
6	**1**	500	0.82	1.21	81.6	43.2	1.1	8.2	85	129	247

[a]General conditions: scandium complex 10 μmol, [**Sc**]/[Ph_3C][$B(C_6F_5)_4$]/[Al^iBu_3] = 1/1/10, E = 4 bar, toluene 10 mL, T = 40 °C, t = 40 min. [b]Given in 10^5 g mol_{Sc}^{-1} h^{-1}. [c]Determined by ^1H NMR and ^{13}C NMR spectra. [d]Determined by GPC in 1,2,4-trichlorobenzene at 150 °C against a polystyrene standard. [e]$M_{n,calcd}$ = yield/(moles of initiator). [f]Determined by DSC.

Table 2. Copolymerization of Ethylene with *meta*-Methoxystyrene (or *para*-Methoxystyrene) Catalyzed by Scandium Complexes 1 and 2[a]

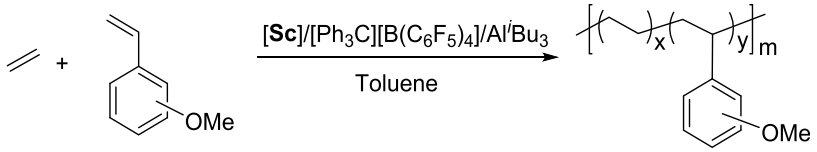

entry	M	Sc	[M]/[Sc]	t (min)	yield (g)	Act.[b]	f_M[c] (mol %)	M_n[d] (×10⁴)	M_w/M_n[d]	T_g[e] (°C)	T_{m1}[e] (°C)	T_{m2}[e] (°C)
1	*m*MOS	**1**	100	20	0.08							
2	*m*MOS	**2**	100	20	0.60 (**P1**)	1.80	3.5	11.4	1.6	−16	106	131
3	*m*MOS	**2**	200	20	0.76 (**P2**)	2.28	5.9	11.6	1.5	−17	95	132
4	*m*MOS	**2**	300	20	0.77 (**P3**)	2.31	7.2	7.1	1.7	−15	87	130
5	*m*MOS	**2**	400	20	0.86 (**P4**)	2.58	9.8	7.3	1.7	−16	78	133
6	*m*MOS	**2**	500	20	0.77 (**P5**)	2.31	11.5	4.7	1.5	−23	58	134
7[f]	*m*MOS	**2**	200	20	0.88	2.64	7.0	4.8	2.0	−14	95	125
8[g]	*m*MOS	**2**	200	20	1.28	3.84	4.3	5.9	2.0	−13	112	132
9	*p*MOS	**1**	200	60	0.16	0.16	9.4	3.5	1.6	−10	82	132
10	*p*MOS	**2**	200	60	0.28	0.28	3.5	5.4	2.8	−5	102	134

[a]General conditions: Scandium complex 10 μmol, [**Sc**]/[Ph_3C][$B(C_6F_5)_4$]/[Al^iBu_3] = 1/1/10, E = 4 bar, toluene 10 mL, T = 40 °C. [b]Given in 10^5 g mol_{Sc}^{-1} h^{-1}. [c]Determined by ^1H NMR and ^{13}C NMR. [d]Determined by GPC in 1,2,4-trichlorobenzene at 150 °C against a polystyrene standard. [e]Determined by DSC. [f]T = 60 °C. [g]T = 80 °C.

ogies, and mechanical and surface properties of resultant E-St^O copolymers are also investigated.

RESULTS AND DISCUSSION

Copolymerization of Ethylene with *ortho*-Methoxystyrene. Methoxystrene (MOS) exists as three isomers, *ortho*-MOS (*o*MOS), *meta*-MOS (*m*MOS), and *para*-MOS (*p*MOS). *o*MOS shows high activity and controllable incorporation during its copolymerization with styrene by using CGC rare-earth complex.[37] First, we examined the copolymerization of *o*MOS with E using **1** (or **2**) in combination with [Ph_3C][$B(C_6F_5)_4$] and Al^iBu_3. Representative results are summarized in Table 1. Complex **1** {(C_7HSMe_4)Sc(CH_2SiMe_3)$_2$(THF)} showed moderate activity (0.34 × 10^5 g mol_{Sc}^{-1} h^{-1}) when [*o*MOS]/[Sc] feed ratio was 100:1 at 4 bar of E in toluene at 40 °C, yielding the copolymer with 14.3 mol % incorporation and a melting temperature (T_m) of 135 °C (Table 1, entry 1). The resultant copolymer showed a high number-average molecular weight (M_n 6.2 × 10^4 g mol^{-1}) with narrow molecular weight distribution (M_w/M_n 1.1). The introduction of a phenyl and a trimethylsilyl group with large steric hindrance and electron-withdrawing properties in complex **2** could endow the catalyst with better catalytic performance, and gave the copolymer with higher incorporation (30.3 mol %) under similar conditions (Table 1, entry 2). To get E-*o*MOS copolymers with a wide range of incorporation, we used complex **1** as the catalyst and carried out the E/*o*MOS copolymerization under varying [*o*MOS]/[**1**] feed ratios from 200:1, 300:1, and 400:1 to 500:1 under 4 bar of E in toluene (Table 1, entries 3−6). Activity slightly increased from 0.50 × 10^5 to 1.29 × 10^5 g mol_{Sc}^{-1} h^{-1}. However, the M_n's of the E-*o*MOS copolymers determined by GPC were higher than the theoretical $M_{n,calcd}$'s, which might be attributed to the partial deactivation of complex **1** caused by the poisoning effect of the polar monomer, especially at high [*o*MOS]/[**Sc**] feeding ratios. Solvent extraction experiments (2-butanone and tetrahydrofuran as eluents) and the narrow distributions of the copolymers in the GPC curves confirmed that all of the resultant products were E-*o*MOS copolymers without homopolymers. The *o*MOS incorporation was increased and ranged from 14.3 to 81.6 mol % (Table 1, entries 1, 3−6). These copolymers showed glass-transition temperature (T_g) around 84−88 °C higher than room

https://doi.org/10.1021/acs.macromol.5c00949
Macromolecules 2025, 58, 6844−6853

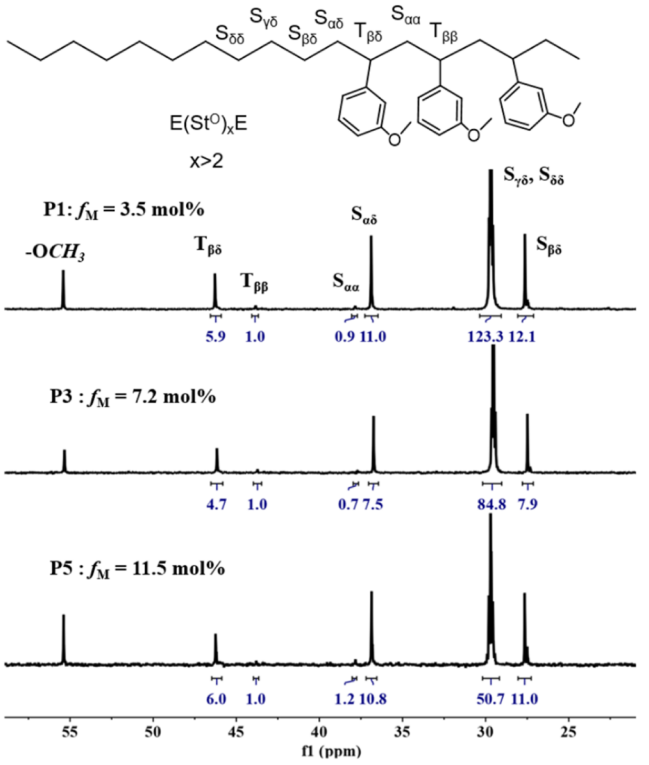

Figure 2. Aliphatic region of ^{13}C NMR spectrum (100 MHz, $C_2D_2Cl_4$, 110 °C) of E-*m*MOS copolymer (Table 2, entries 2, 4, and 6).

temperature and two T_m's around 129−136 °C for continuous PE segments on copolymers and 241−247 °C for long continuous *o*MOS segments on copolymers and behave like plastics, not elastomers.

The ^{13}C nuclear magnetic resonance (NMR) spectrum of the representative copolymers (Figures S2, S6, S12, and S14) with *o*MOS contents of 14.3, 48.2, 69.0, and 81.6 mol % indicates that they are diblock.[31,36] Both long continuous *o*MOS-*o*MOS segments and long continuous ethylene−ethylene sequences are hard chains, and then behave as plastics (see the SI for detailed NMR analysis). The competitive reactivity ratios (r_{oMOS} = 6.06, r_E = 0.21) were calculated according to the Fineman−Ross equation at low monomer conversion (<10%), which further explained that the *o*MOS insertion into Sc−C bonds took place faster than ethylene, and then favorably formed long continuous *o*MOS-*o*MOS segments (Figure S68). The reason might be that the self-activated phenomenon occurred during *o*MOS polymerization. With the consumption of *o*MOS, longer continuous E−E segments formed. Similar copolymers with gradient chain structure were observed in scandium-catalyzed styrene polymerization.[38−40]

Ethylene/*meta*-Methoxystyrene and Ethylene/*para*-Methoxystyrene Copolymerizations. If the MOS activity becomes weak and matches with ethylene, then we could easily regulate the micromolecular structure and probably obtain E-MOS copolymers with soft/hard alternating microstructures that are characteristic of TPEs. Methoxy groups located in different positions of MOS could affect the intermolecular coordination among O atom, vinyl group, and catalyst metal center, which further influences the polymerization activity and incorporation.[41,42] We studied the E/*m*MOS and E/*p*MOS copolymerization subsequently (Table 2). Both complexes **1** and **2** show very low activity for *m*MOS and *p*MOS homopolymerization in the absence of E (Table S1). Next, we examined the copolymerization of ethylene with *m*MOS. Complex **1** showed almost no activity for E/*m*MOS copolymerization (Table 2, entry 1), which was different from the result for E/*o*MOS copolymerization (Table 1, entry 1).

Switching to complex **2** with large steric hindrance and electron-withdrawing groups, better results were found under the same conditions. E-*m*MOS copolymer with higher activity (1.80×10^5 g mol_{Sc}^{-1} h^{-1}), lower polar monomer incorporation (3.5 mol %), and high M_n (11.4×10^4 g mol^{-1}) were obtained when the [*m*MOS]/[**2**] feed ratio was 100:1 under 4 bar of E at 40 °C in toluene (Table 2, entry 2). This further confirms that the coordination between the methoxy group in the *meta*-position and the Sc center is weaker. With [*m*MOS]/[**2**] feed ratios raising to 200:1, 300:1, 400:1, and 500:1 from 100:1, the comonomer incorporation increased to 5.9, 7.2, 9.8, and 11.5 from 3.5 mol %, while the M_n decreased from 11.6×10^4 g mol^{-1} to 4.7×10^4 g mol^{-1} (Table 2, entries 3−6), indicating that chain transfer to

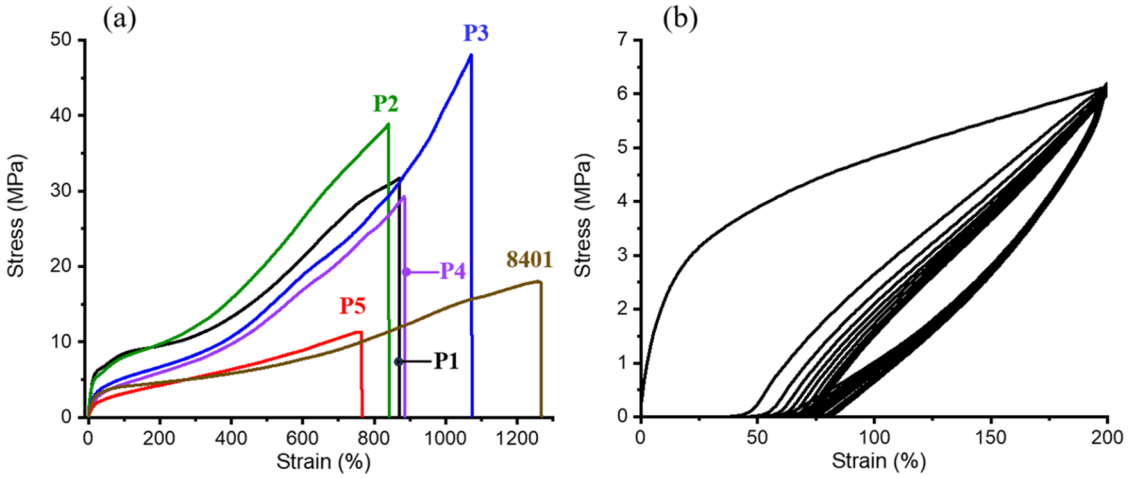

Figure 3. (a) Stress−strain curves measured at a speed of 50 mm min^{-1}. (b) Hysteresis curves of the copolymer **P3**. Ten cycles at successive stretching with 200% strain were performed.

https://doi.org/10.1021/acs.macromol.5c00949
Macromolecules 2025, 58, 6844−6853

Table 3. Mechanical Properties of E-*m*MOS Copolymers with Different Polar Comonomer Incorporation Ratios and POE of 8401

entry	E-*m*MOS	f_M (mol %)	T_{m1} (°C)	M_n (×10^4)	stress (MPa)	strain (%)	elastic modulus
1	**P1**	3.5	106	11.4	31.7 ± 2.3	870 ± 2.9	52.2 ± 1.8
2	**P2**	5.9	95	11.6	38.9 ± 1.9	840 ± 3.4	47.8 ± 2.6
3	**P3**	7.2	87	7.1	48.1 ± 1.5	1073 ± 3.8	28.6 ± 2.4
4	**P4**	9.8	78	7.3	29.3 ± 2.5	886 ± 3.2	19.7 ± 3.9
5	**P5**	11.5	58	4.7	11.4 ± 4.3	770 ± 3.9	12.0 ± 4.5
6	**POE-8401**	14.7	80	9.7	18.0 ± 4.1	1268 ± 6.5	31.5 ± 5.2

comonomer possibly occurred at high *m*MOS feeding. Similar results were found in the half-sandwich scandium complex catalyzed styrene polymerization in the presence of anisoles.[43] E-*m*MOS copolymers showed one T_g and two T_m's (Table 2, entries 2−6). The T_g values of E-*m*MOS copolymers ranged from −15 to −23 °C. The lower T_{m1} values of E-*m*MOS copolymers decreased from 106 to 58 °C as the *m*MOS incorporation increased from 3.5 to 11.5 mol %, and the higher T_{m2} values remained almost unchanged (around 130 °C). These T_g and bis-T_ms values are different from the previously reported amorphous alternating[31] and pseudo-random[36,44] ethylene-styrene derivates copolymer, which is due to the fact that these new E-*m*MOS copolymers have special chain structures and comonomer sequence distributions (see details below). To investigate the temperature effect for copolymerization, we then carried out the E/*m*MOS copolymerization at 60 and 80 °C (Table 2, entries 7−8). As the temperature increased, the activities rose to 2.64 × 10^5 and 3.84 × 10^5 from 2.28 × 10^5 g mol$_{Sc}^{-1}$ h^{-1} (Table 2, entries 3, 7, and 8). The comonomer incorporation ratios showed a trend of first rising (7.0 mol %) and then falling (4.3 mol %), which also influenced the values of T_g and T_m. E-*m*MOS copolymers with various *m*MOS incorporation (7.0, 4.3, and 5.9 mol %) showed complicated T_m combinations 95/125, 112/132, and 95/132 °C (Table 2, entries 3, 7, and 8). This data indicates that the T_m values are not affected by the comonomer incorporation but probably also by the comonomer sequence distribution. The TGA of E-*m*MOS copolymers demonstrated the thermal decomposition at $T_{5\%}$ = 414−427 °C ($T_{5\%}$, defined as the temperature of 5% weight loss in the TGA curve), suggesting the homogeneity in chemical composition and thermostability of the obtained copolymers with various *m*MOS incorporations (Table 2, entries 2−6, Figures S63−S67).

To get more information about the comonomer effect toward polymerization, we carried out the E/*p*MOS copolymerization under similar conditions. Both complexes **1** and **2** showed a good catalytic effect during the copolymerization process. Complex **1** yielded E-*p*MOS copolymer with higher *p*MOS content (9.4 mol %) and lower M_n (3.5 × 10^4 g mol^{-1}) compared with **2** (3.5 mol % incorporation and M_n 5.4 × 10^4 g mol^{-1}, entries 9−10 in Table 2). Low *p*MOS incorporation at a certain range could lead to the formation of longer continuous E−E segments, and then give higher T_{m1}. Then, E-*p*MOS copolymer produced by **1** shows lower T_g (−10) and T_{m1} (82 °C) compared with **2** (T_g −5, T_{m1} 102 °C, entries 9−10). The activity of E-*p*MOS copolymerization was the lowest in comparison with E/*o*MOS and E/*m*MOS copolymerization under similar conditions, because OMe on *p*MOS was far away from the vinyl group and then showed the weakest activated effect for polymerization. Complexes **1** and **2** showed low activity and low M_n for E/*p*MOS copolymerization, then we studied the structures and properties of E/*m*MOS copolymers in detail.

To further get detailed chain structures, we analyzed the ^{13}C NMR spectra of the representative E-*m*MOS copolymers with various incorporations (3.5, 7.2, and 11.5 mol %) shown in Figure 2 (Table 2, entries 2, 4, and 6). No signals are observed at around δ = 25.2 ppm ($S_{\beta\beta}$ on {EE-St^O-EE} unit) and 44.7 ppm ($T_{\delta\delta}$ on {-St^O-E-St^O-} and {-EE-St^O-EE-} units), indicating that the alternative and discrete structures for *m*MOS are absent and hard to form during polymerization.[29,30,36,44] The resonance at δ = 29.7 ppm is attributed to the methylene carbon atoms ($S_{\gamma\delta}$, $S_{\delta\delta}$) for a certain length of E−E sequences, and the peaks at δ = 43.8 ppm ($T_{\beta\beta}$) and 37.8 ppm ($S_{\alpha\alpha}$) arise from continuous *m*MOS segments $(St^O)_x$. Moreover, the signals for the connection points of two blocky segments $(E)_y$ and $(St^O)_x$ are also observed ($T_{\beta\delta}$ 45.8 ppm, $S_{\alpha\delta}$ 36.9 ppm, and $S_{\beta\delta}$ 27.6 ppm), proving the formation of multiblock-like structure. Competitive reactivity ratios for E/*m*MOS copolymerization were calculated according to the Fineman−Ross equation at low monomer conversion (<10%) further illuminating that it is favorable to give block-like structures, and the lengths of $(E)_y$ are longer than those of $(St^O)_x$ that is consistent with NMR analysis (r_E = 2.6, r_{mMOS} = 1.1, Figure S69). In addition, the SSA-DSC curve of the E-*m*MOS copolymer synthesized under low *m*MOS conversion (7.3%) further proved that the hard segments were formed during the whole copolymerization process, not when *m*MOS had been depleted. E-*m*MOS are multiblock-like copolymers, which is consistent with the reactivity ratios data (see details in Figure S70). Therefore, these novel multiblock-like E-*m*MOS copolymers are composed of short $(St^O)_x$ units and a series of $(E)_y$ segments with different lengths.

Mechanical and Surface Properties of E-*m*MOS Copolymers. E-*m*MOS copolymers have T_g values (−13 to −23 °C) lower than room temperature and might behave as TPE-Os. The stress−strain curves and mechanical properties of E-*m*MOS copolymers (**P1**−**P5** in Table 2) and commercially available POE 8401 are shown in Figure 3 (a) and Table 3. **P1** (3.5 mol % incorporation) showed a typical feature of elastomer, exhibiting the mechanical property with a high strain value at 870% under a stress-at-break value of 31.7 MPa. With the increase of *m*MOS incorporation ratios, **P2** (5.9 mol % incorporation) and **P3** (7.2 mol % incorporation) showed closed (or better) strain values (840% for **P2**, 1073% for **P3**) and elevated stress-at-break values (38.9 MPa for **P2**, 48.1 MPa for **P3**). **P4** (9.8 mol % incorporation) showed similar strain (886%) but poor stress-at-break (29.3 MPa) compared with **P1**. **P5** (11.5 mol % incorporation) had the worst mechanical properties (770% strain and 11.4 MPa stress-at-break). To investigate the elastic recovery property, **P3** was subjected to hysteresis testing, in which each specimen was extended to 200% elongation for ten cycles (Figure 3(b)). It

https://doi.org/10.1021/acs.macromol.5c00949
Macromolecules 2025, 58, 6844−6853

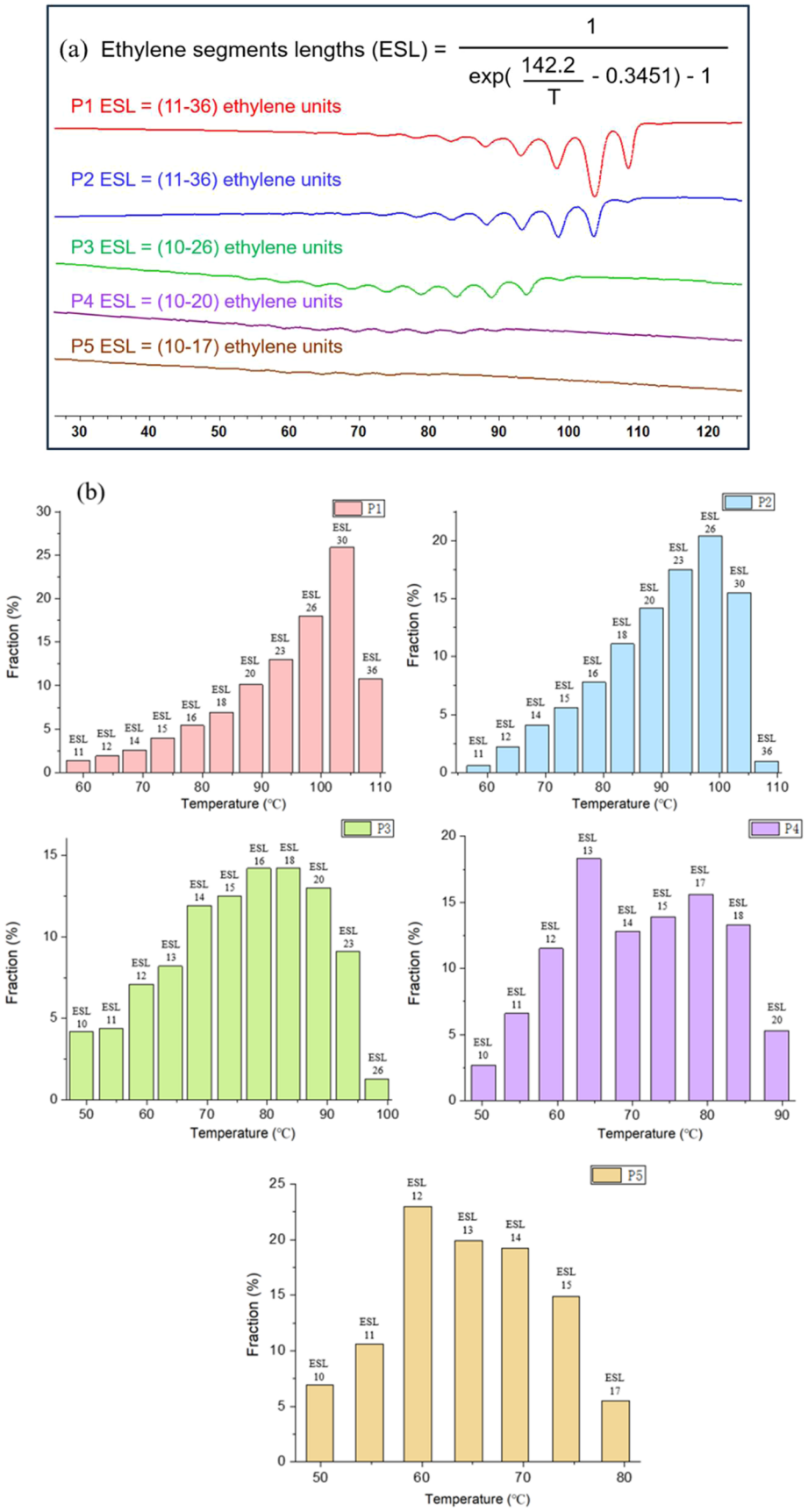

Figure 4. (a) DSC traces of **P1**−**P5** determined after a successive self-nucleation and annealing (SSA) procedure. (b) Histogram of the distribution and fraction of ethylene segment lengths (ESL) of **P1**−**P5** based on peak deconvolution of the SSA curves.

https://doi.org/10.1021/acs.macromol.5c00949
Macromolecules 2025, 58, 6844−6853

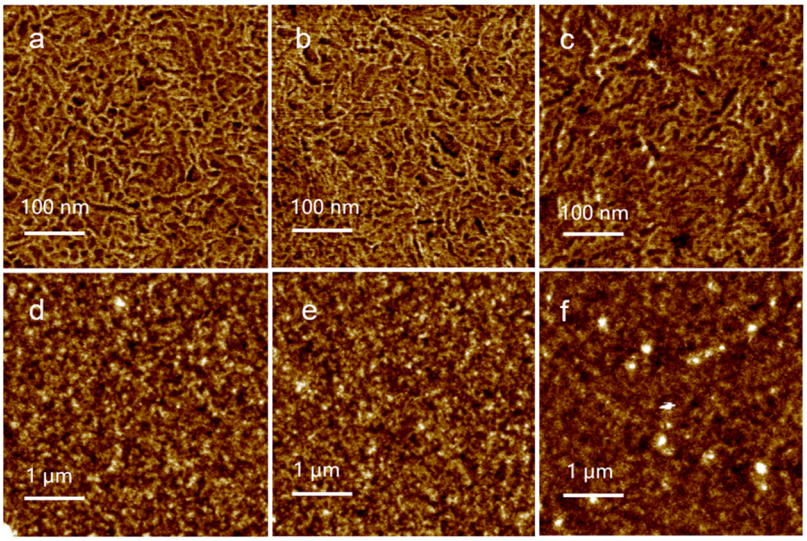

Figure 5. AFM phase and height images of the E-*m*MOS copolymers. AFM phase (a) and height (d) images of **P1**. AFM phase (b) and height (e) images of **P2**. AFM phase (c) and height (f) images of **P3**.

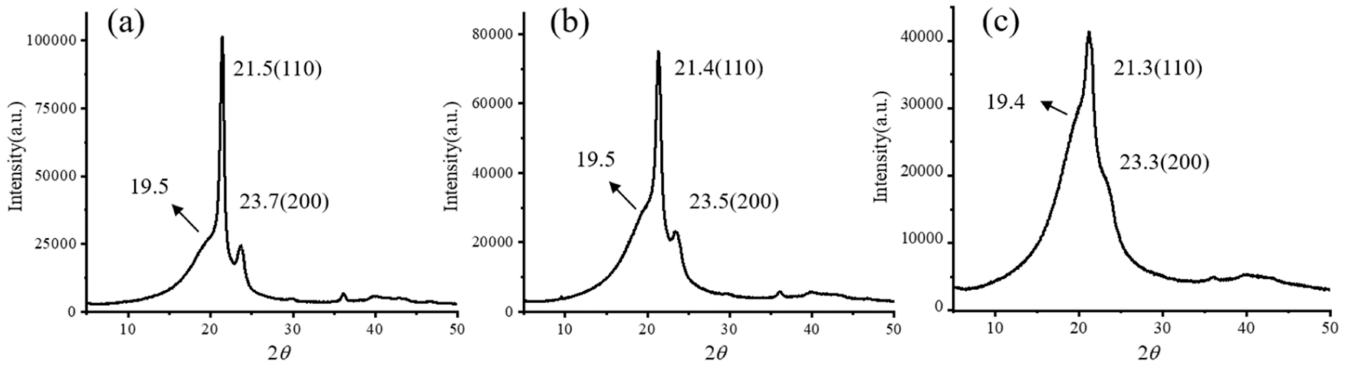

Figure 6. Wide-angle X-ray scattering (WAXD) profiles of the E-*m*MOS copolymers at 25 °C. (a) **P1** (f_M = 3.5 mol %); (b) **P2** (f_M = 5.9 mol %); (c) **P3** (f_M = 7.2 mol %).

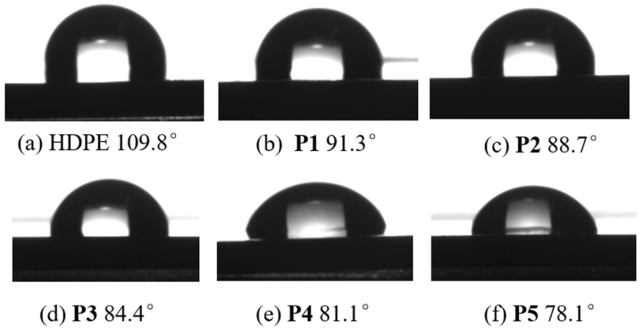

Figure 7. Water contact angles (WCA) of HDPE and E-*m*MOS copolymers. (a) HDPE; (b) **P1** (f_M = 3.5 mol %); (c) **P2** (f_M = 5.9 mol %); (d) **P3** (f_M = 7.2 mol %); (e) **P4** (f_M = 9.8 mol %); (f) **P5** (f_M = 11.5 mol %).

showed an excellent elastic recovery. We could find that there was a certain amount of the unrecovered strain after the first cycle in **P3**, followed by minimal deformation in the next nine cycles, indicating that a permanent structural change happened during the first cycle, after which better elastomer properties were created. In order to make these results clear, we carried out successive self-nucleation annealing (SSA) treatments on **P1**−**P5** samples. SSA-DSC curves showed several obvious endothermal peaks, and the corresponding ethylene sequence lengths (ESL) of **P1**−**P5** were calculated according to the equation in Figure 4.[33,45]

The ESLs of **P1**−**P5** copolymers are distinguishing (Figure 4). ESL values of **P1** to **P5** decreased with the increase of *m*MOS incorporation. **P3** showed the best mechanical properties, indicating that its ESL was the most suitable. **P1** and **P2** consisted of longer continuous ethylene segments, and the major parts of their ESLs were around 26−30. **P3** had moderate ESL (10−26), and the distribution was almost normal, resulting in the mutual matching between "hard segments" (different lengths of ethylene segments) and "soft segments" (short continuous *m*MOS-*m*MOS sequences), which endowed it with high stress-at-break and high strain. The mechanical properties of **P1**−**P3** are superior to many polyolefin-based TPEs having been reported,[46−48] and are competitive to those of commercial ethylene-styrene interpolymers (ESIs) (such as ES16, f_{St} = 4.7 mol %, 31.7 MPa for stress-at-break, 666% for strain).[49] **P4** and **P5** had shorter average ESL values compared with **P3**, causing the decline in the crystalline ability of ethylene segments as "hard segments" and leading to lower strength. Compared with the hydrophobic thermoplastic elastomer composed of soft ethylene-fluorostyrene segments and hard crystalline ethylene−ethylene segments (39.5 MPa stress and 774% strain-at-break),[36] E-*m*MOS

https://doi.org/10.1021/acs.macromol.5c00949
Macromolecules 2025, 58, 6844−6853

copolymers with multiblock-like hard/soft microstructures exhibit superior mechanical properties.

To study the phase structures of E-*m*MOS copolymers, we carried out atomic force microscope (AFM, Figure 5) and wide-angle X-ray scattering (WAXD, Figure 6) experiments for **P1**−**P3**. The AFM images presented clear phase separation arising from the incompatibility between short *meta*-methoxystyrene segments and different lengths of ethylene sequences. In the WAXD profile, a strong diffraction peak appeared at about 21.4° and a weak diffraction peak observed at approximately 23.5° might be respectively assigned to the (110) and (200) lattice planes of ethylene segments,[50−53] while the shoulder peak observed at around 19.5° might be arising from the amorphous region of consecutive *meta*-methoxystyrene sequences.[36,48] These characterizations of copolymers' microstructures reveal that the excellent mechanical properties of E-*m*MOS copolymers are attributed to the novel multiblock-like sequences which contain short consecutive *meta*-methoxystyrene (soft segments) and a series of ethylene sequences with different lengths (hard parts).

The surface properties of these polymers were studied by water contact angle (WCA) experiments, which showed that the hydrophilicity of E-*m*MOS copolymers was significantly raised due to the incorporation of polar groups (Figure 7). Compared with pure polyethylene (WCA 109.8°), E-*m*MOS copolymers showed smaller WCA values from 91.3° (**P1**) to 78.1° (**P5**). The high content of polar monomers in the copolymers contributed to their much lower WCA values. This result indicates that the insertion of polar monomer immensely improves the surface properties of these polyolefin materials, which may have great application prospects in adhesion, dyeability, conductivity, and compatibility with other polar materials.

CONCLUSIONS

We have achieved, for the first time, controlled copolymerization of ethylene (E) and *meta*-methoxystyrene (*m*MOS) by using a heterocyclic-fused cyclopentadienyl scandium complex such as **2**. The copolymerization has led to the formation of unique multiblock-like copolymers composed of relatively long crystalline E−E segments (hard) and short amorphous *m*MOS-*m*MOS sequences (soft). The copolymer products behave as thermoplastic elastomers and show high mechanical properties depending on their chain sequence structure (*m*MOS incorporation and ethylene segments lengths (ESLs)) and molecular weight, as demonstrated by **P1**−**P5** samples. **P3** with suitable ESLs (10−26) and M_n (7.1×10^4 g mol^{-1}) has the highest tensile strength (48.1 MPa) and highest toughness (1073%). These samples have T_g (−15 to −23 °C) lower than room temperature and two T_m's (58−106 and around 130 °C) adjusted by their chain structures, whereas E-*o*MOS copolymers behave as plastics. In addition, E-*m*MOS copolymers show improved hydrophilic surface properties with water contact angles ranging from 91.3 to 78.1° compared with pure polyethylene (109.8°). The excellent properties, including high elasticity, high toughness, and high hydrophilicity, along with the ease of synthesis from readily available starting materials may enable this series of new thermoplastic elastomer materials to find a wide range of practical applications in the future. Moreover, this work may also help design new catalysts and new functional polyolefins.

ASSOCIATED CONTENT

Supporting Information

The Supporting Information is available free of charge at https://pubs.acs.org/doi/10.1021/acs.macromol.5c00949.

Additional experimental and analysis details include homopolymerization of MOS; polymer characterization (^{1}H, ^{13}C and DEPT135 NMR, DSC, GPC, and TGA); and Fineman−Ross plot for the copolymerization of E and MOS (PDF)

AUTHOR INFORMATION

Corresponding Author

Baoli Wang − *State Key Laboratory of Polymer Science and Technology, Changchun Institute of Applied Chemistry, Chinese Academy of Sciences, Changchun 130022, China; School of Applied Chemistry and Engineering, University of Science and Technology of China, Hefei 230026, China;* orcid.org/0000-0001-5057-2339; Email: wang@ciac.ac.cn

Authors

Hui Tian − *State Key Laboratory of Polymer Science and Technology, Changchun Institute of Applied Chemistry, Chinese Academy of Sciences, Changchun 130022, China; School of Applied Chemistry and Engineering, University of Science and Technology of China, Hefei 230026, China*

Chunji Wu − *State Key Laboratory of Polymer Science and Technology, Changchun Institute of Applied Chemistry, Chinese Academy of Sciences, Changchun 130022, China*

Dongmei Cui − *State Key Laboratory of Polymer Science and Technology, Changchun Institute of Applied Chemistry, Chinese Academy of Sciences, Changchun 130022, China; School of Applied Chemistry and Engineering, University of Science and Technology of China, Hefei 230026, China;* orcid.org/0000-0001-8372-5987

Complete contact information is available at: https://pubs.acs.org/10.1021/acs.macromol.5c00949

Notes

The authors declare no competing financial interest.

ACKNOWLEDGMENTS

This work was partially supported by the National Natural Science Foundation of China (project Nos 52273017, 22331010, U21A20279, and 52273016) and Natural Science Foundation of Jilin Province (No. SKL202302033).

REFERENCES

(1) Müller, G.; Rieger, B. Propene based thermoplastic elastomers by early and late transition metal catalysis. *Prog. Polym. Sci.* **2002**, *27*, 815−851.

(2) Wang, W.; Lu, W.; Goodwin, A.; Wang, H.; Yin, P.; Kang, N.-G.; Hong, K.; Mays, J. W. Recent advances in thermoplastic elastomers from living polymerizations: Macromolecular architectures and supramolecular chemistry. *Prog. Polym. Sci.* **2019**, *95*, 1−31.

(3) Chittella, H.; Yoon, L. W.; Ramarad, S.; Lai, Z.-W. Rubber waste management: A review on methods, mechanism, and prospects. *Polym. Degrad. Stab.* **2021**, *194*, No. 109761.

(4) Pan, C.; Shi, Z.; Zhang, R.; Liu, P. Metathetic degradation of waste vulcanized emulsion type butadiene-based rubber. *Polym. Degrad. Stab.* **2024**, *225*, No. 110780.

(5) Drobny, J. G.Recent Developments and Trends. In *Handbook of Thermoplastic Elastomers*; William Andrew Inc., 2014; pp 341−345.

(6) Whelan, D.Thermoplastic Elastomers. In *Brydson's Plastics Materials*; Elsevier, 2017; pp 653−703.
(7) Spontak, R. J.; Patel, N. P. Thermoplastic Elastomers: Fundamentals and Applications. *Curr. Opin. Colloid Interface Sci.* **2000**, *5*, 334−341.
(8) Drobny, J. G.Thermoplastic Polyurethane Elastomers. In *Handbook of Thermoplastic Elastomers*; William Andrew, 2014; pp 233−253.
(9) Drobny, J. G.Styrenic Block Copolymers. In *Handbook of Thermoplastic Elastomers*; William Andrew, 2014; pp 175−194.
(10) Sun, M.; Xiao, Y.; Liu, K.; Yang, X.; Liu, P.; Jie, S.; Hu, J.; Shi, S.; Wang, Q.; Lim, K. H.; Liu, Z.; Li, B.-G.; Wang, W.-J. Synthesis and characterization of polyolefin thermoplastic elastomers: A review. *Can. J. Chem. Eng.* **2023**, *101*, 4886−4906.
(11) Zhu, L.; Yu, H.; Wang, L.; Xing, Y.; Amin, B. U. Advances in the synthesis of polyolefin elastomers with "chain-walking" catalysts and electron spin resonance research of related catalytic systems. *Curr. Org. Chem.* **2021**, *25*, 935−949.
(12) Zanchin, G.; Leone, G. Polyolefin thermoplastic elastomers from polymerization catalysis: Advantages, pitfalls and future challenges. *Prog. Polym. Sci.* **2021**, *113*, No. 101342.
(13) Mohite, A. S.; Rajpurkar, Y. D.; More, A. P. Bridging the gap between rubbers and plastics: a review on thermoplastic polyolefin elastomers. *Polym. Bull.* **2022**, *79*, 1309−1343.
(14) Arriola, D. J.; Carnahan, E. M.; Hustad, P. D.; Kuhlman, R. L.; Wenzel, T. T. Catalytic production of olefin block copolymers via chain shuttling polymerization. *Science* **2006**, *312*, 714−719.
(15) Zintl, M.; Rieger, B. Novel Olefin block copolymers through chain-shuttling polymerization. *Angew. Chem., Int. Ed.* **2007**, *46*, 333−335.
(16) Valente, A.; Stoclet, G.; Bonnet, F.; Mortreux, A.; Visseaux, M.; Zinck, P. Isoprene−styrene chain shuttling copolymerization mediated by a Lanthanide half-sandwich complex and a Lanthanidocene: straightforward access to a new type of thermoplastic elastomers. *Angew. Chem., Int. Ed.* **2014**, *53*, 4638−4641.
(17) Baulu, N.; Langlais, M.; Ngo, R.; Thuilliez, J.; Jean-Baptiste-dit-Dominique, F.; D'Agosto, F.; Boisson, C. Switch from anionic polymerization to coordinative chain transfer polymerization: a valuable strategy to make olefin block copolymers. *Angew. Chem., Int. Ed.* **2022**, *61*, No. e202204249.
(18) Langlais, M.; Baulu, N.; Dronet, S.; Dire, C.; Jean-Baptiste-dit-Dominique, F.; Albertini, D.; D'Agosto, F.; Montarnal, D.; Boisson, C. Multiblock copolymers based on highly crystalline polyethylene and soft poly(ethylene-co-butadiene) segments: towards polyolefin thermoplastic elastomers. *Angew. Chem., Int. Ed.* **2023**, *62*, No. e202310437.
(19) Pan, L.; Zhang, K.; Nishiura, M.; Hou, Z. Chain-shuttling polymerization at two different scandium sites: regio- and stereospecific "one-pot" block copolymerization of styrene, isoprene, and butadiene. *Angew. Chem., Int. Ed.* **2011**, *50*, 12012−12015.
(20) Dau, H.; Jones, G. R.; Tsogtgerel, E.; Nguyen, D.; Keyes, A.; Liu, Y.-S.; Rauf, H.; Ordonez, E.; Puchelle, V.; Alhan, H. B.; Zhao, C.; Harth, E. Linear block copolymer synthesis. *Chem. Rev.* **2022**, *122*, 14471−14553.
(21) Zhang, Y.; Keaton, R. J.; Sita, L. R. Degenerative transfer living Ziegler-Natta polymerization: application to the synthesis of monomodal stereoblock polyolefins of narrow polydispersity and tunable block length. *J. Am. Chem. Soc.* **2003**, *125*, 9062−9069.
(22) Coates, G. W.; Waymouth, R. M. Oscillating Stereocontrol: a strategy for the synthesis of thermoplastic elastomeric polypropylene. *Science* **1995**, *267*, 217−219.
(23) Lee, J. C.; Park, K. L.; Bae, S. M.; Lee, H. J.; Baek, J. W.; Lee, J.; Sa, S.; Shin, E. J.; Lee, K. S.; Lee, B. Y. Styrene moiety-carrying diorganozinc compound preparation for polystyrene-poly(ethylene-co-1-hexene)-polystyrene triblock copolymer production. *Macromolecules* **2020**, *53*, 7274−7284.
(24) Biswas, A.; Singha, N. K.; Bhowmick, A. K. Effect of polar modifications on cure characteristics, solvent resistance and thermomechanical properties of metallocene-based polyolefinic elastomers. *Eur. Polym. J.* **2010**, *46*, 364−373.
(25) Dong, J. Y.; Hong, H.; Chung, T. C.; et al. Synthesis of linear polyolefin elastomers containing divinylbenzene units and applications in cross-linking, functionalization, and graft reactions. *Macromolecules* **2003**, *36*, 6000−6009.
(26) Micheletti, C.; Soldati, L.; Weder, C.; Pucci, A.; Clough, J. M. Mechanochromic polyolefin elastomers. *ACS Appl. Polym. Mater.* **2024**, *6*, 6572−6580.
(27) Schneider, Y.; Lynd, N. A.; Kramer, E. J.; Bazan, G. C. Novel elastomers prepared by grafting *n*-butyl acrylate from polyethylene macroinitiator copolymers. *Macromolecules* **2009**, *42*, 8763−8768.
(28) Wang, Q.; Chen, M.; Zou, C.; Chen, C. Direct synthesis of polar-functionalized polyolefin elastomers. *Angew. Chem., Int. Ed.* **2025**, *64* (20), No. e202423814.
(29) Cui, L.; Chen, M.; Chen, C.; Liu, D.; Jian, Z. Systematic studies on (co)polymerization of polar styrene monomers with palladium catalysts. *Macromolecules* **2019**, *52*, 7197−7206.
(30) Zhang, Z.; Jiang, Y.; Lei, R.; Zhang, Y.; Li, S.; Cui, D. Proximity-driven synergic copolymerization of ethylene and polar monomers. *Macromolecules* **2023**, *56*, 2476−2483.
(31) Li, S.; Liu, D.; Wang, Z.; Cui, D. Development of group 3 catalysts for alternating copolymerization of ethylene and styrene derivatives. *ACS Catal.* **2018**, *8*, 6086−6093.
(32) Chen, R.; Yao, C.; Wang, M.; Xie, H.; Wu, C.; Cui, D. Synthesis of heterocyclic-fused cyclopentadienyl scandium complexes and the catalysis for copolymerization of ethylene and dicyclopentadiene. *Organometallics* **2015**, *34*, 455−461.
(33) Wu, C.; Liu, B.; Lin, F.; Wang, M.; Cui, D. *cis*-1,4-Selective copolymerization of ethylene and butadiene: a compromise between two mechanisms. *Angew. Chem., Int. Ed.* **2017**, *56*, 6975−6979.
(34) Tian, H.; Wang, Y.; Wu, C.; Wang, B. A compatibilizing strategy for upcycling polyethylene and polystyrene with ethylene/(phenyl functionalized α-olefin) copolymers containing continuous comonomer segments. *Macromolecules* **2024**, *57*, 6275−6283.
(35) Tian, H.; Wang, Y.; Wu, C.; Kang, X.; Wang, B. Direct synthesis of polyethylene containing two kinds of heteroatoms by scandium complexes. *Polym. Chem.* **2025**, *16*, 1057−1064.
(36) Wang, T.; Wu, C.; Ji, X.; Cui, D. Direct Synthesis of functional thermoplastic elastomer with excellent mechanical properties by scandium-catalyzed copolymerization of ethylene and fluorostyrenes. *Angew. Chem., Int. Ed.* **2021**, *60*, 25735−25740.
(37) Liu, D.; Wang, M.; Wang, Z.; Wu, C.; Pan, Y.; Cui, D. Stereoselective copolymerization of unprotected polar and nonpolar styrenes by an yttrium precursor: control of polar-group distribution and mechanism. *Angew. Chem., Int. Ed.* **2017**, *56*, 2714−2719.
(38) Deng, P.; Sang, L.; Gong, X.; Guo, X.; Cheng, J. Syndiotactic (co)polymerization of 4-vinylbenzocyclobutene catalyzed by rare-earth metal complex. *Macromolecules* **2024**, *57*, 6166−6176.
(39) Liu, W.; Song, Y.-y.; Diao, K. Y.; Guo, F. Copolymerization of myrcene with styrene catalyzed by half-sandwich scandium complexes. *Acta Polym. Sin.* **2019**, *50*, 957−963.
(40) Lin, F.; Wang, M.; Pan, Y.; Tang, T.; Cui, D.; Liu, B. Sequence and regularity controlled coordination copolymerization of butadiene and styrene: strategy and mechanism. *Macromolecules* **2017**, *50*, 849−856.
(41) Liu, D.; Yao, C.; Wang, R.; Wang, M.; Wang, Z.; Wu, C.; Lin, F.; Li, S.; Wan, X.; Cui, D. Highly isoselective coordination polymerization of *ortho*-methoxystyrene with β-diketiminato rare-earth-metal precursors. *Angew. Chem., Int. Ed.* **2015**, *54*, 5205−5209.
(42) Wang, F.; Wang, X.-l.; Pan, L.; Mao, X.-h.; Wu, H.-y.; Li, Y.-S. Copolymerization of ethylene with polar styrene monomers catalyzed by phosphino-dihydronaphtholate neutral nickel catalysts. *J. Polym. Sci.* **2024**, *62*, 2058−2070.
(43) Yamamoto, A.; Nishiura, M.; Oyamada, J.; Koshino, H.; Hou, Z. Scandium-catalyzed syndiospecific chain-transfer polymerization of styrene using anisoles as a chain transfer agent. *Macromolecules* **2016**, *49*, 2458−2466.

https://doi.org/10.1021/acs.macromol.5c00949
Macromolecules 2025, 58, 6844−6853

(44) Liu, B.; Qiao, K.; Fang, J.; Wang, T.; Wang, Z.; Liu, D.; Xie, Z.; Maron, L.; Cui, D. Mechanism and effect of polar styrenes on scandium-catalyzed copolymerization with ethylene. *Angew. Chem., Int. Ed.* **2018**, *57*, 14896−14901.
(45) Fillon, B.; Wittmann, J. C.; Lotz, B.; Thierry, A. Self-nucleation and recrystallization of isotactic polypropylene (α phase) investigated by differential scanning calorimetry. *J. Polym. Sci., Part B:Polym. Phys.* **1993**, *31*, 1383−1393.
(46) Bi, Z.; Zhou, J.; Zhu, N.; Peng, D.; Chen, C. Heterogeneous nickel catalysts for the synthesis of ethylene-based polyolefin elastomers. *Macromolecules* **2024**, *57*, 1080−1086.
(47) Chen, C.; Chen, M.; Wang, Z. Catalytic synthesis of polyolefin elastomer using unsymmetrical α-diimine nickel catalyst. *Acta Chim. Sin.* **2023**, *81*, 559−564.
(48) Wang, H.; Yang, Y.; Nishiura, M.; Higaki, Y.; Takahara, A.; Hou, Z. Synthesis of self-healing polymers by scandium-catalyzed copolymerization of ethylene and anisylpropylenes. *J. Am. Chem. Soc.* **2019**, *141*, 3249−3257.
(49) Chen, H.; Guest, M. J.; Chum, S.; Hiltner, A.; Baer, E. Classification of ethylene-styrene interpolymers based on comonomer content. *J. Appl. Polym. Sci.* **1998**, *70*, 109−119.
(50) Mark, J. E. *Physical Properties of Polymers Handbook*; Springer: New York, 2007.
(51) McDaniel, P. B.; Deitzel, J. M.; Gillespie, J. W. Structural hierarchy and surface morphology of highly drawn ultra-high molecular weight polyethylene fibers studied by atomic force microscopy and wide-angle X-ray diffraction. *Polymer* **2015**, *69*, 148−158.
(52) Yeh, J.-T.; Lin, S.-C.; Tu, C.-W.; Hsie, K.-H.; Chang, F.-C. Investigation of the drawing mechanism of UHMWPE fibers. *J. Mater. Sci.* **2008**, *43*, 4892−4900.
(53) Zhu, B.; Liu, J.; Wang, T.; Han, M.; Valloppilly, S.; Xu, S.; Wang, X. Novel polyethylene fibers of very high thermal conductivity enabled by amorphous restructuring. *ACS Omega* **2017**, *2*, 3931−3944.

https://doi.org/10.1021/acs.macromol.5c00949
Macromolecules 2025, 58, 6844−6853